

Original Paper

Natural gas characteristics and gas-source comparisons of the Lower Triassic Feixianguan Formation, Eastern Sichuan Basin, China



Zi-Yun Zheng^a, Yin-Hui Zuo^{a,*}, Hua-Guo Wen^a, De-Ming Li^a, Yang Luo^b,
Jia-Zhen Zhang^a, Mei-Hua Yang^a, Jian-Cheng Zeng^a

^a State Key Laboratory of Oil and Gas Geology and Exploitation, Chengdu University of Technology, Chengdu, Sichuan, 610059, China

^b PetroChina Southwest Oil & Gas Field Company, Chengdu, Sichuan, 610051, China

ARTICLE INFO

Article history:

Received 24 June 2022

Received in revised form

28 November 2022

Accepted 13 February 2023

Available online 14 February 2023

Edited by Jie Hao and Teng Zhu

Keywords:

Eastern Sichuan Basin
Feixianguan Formation
Natural gas origin
Gas-source comparison
Longtan Formation

ABSTRACT

There is great controversy regarding the origin and source of natural gas in the Lower Triassic Feixianguan Formation in the Eastern Sichuan Basin. This seriously restricts the study of natural gas dynamics in the Feixianguan Formation and thus hampers natural gas exploration in the region, so further study is urgently required. Using experimental tests of natural gas composition, stable isotopes, and noble gas isotopes with gas chromatography (GC) and mass spectrometry (MS) studies of source rock and reservoir asphalt saturated hydrocarbons, the natural gas geochemical characteristics, the genetic identification and a gas-source comparison of the Feixianguan Formation were studied. Then, constrained by the thermal history, the histories of gas generation and expulsion were restored by basin simulation technology. Finally, a gas accumulation model was established for the Feixianguan Formation. The results showed that (1) the H₂S-rich and H₂S-poor gas reservoirs of the Feixianguan Formation are distributed on the east and west sides of the Kaijiang-Liangping trough in the Eastern Sichuan Basin, respectively. The carbon and hydrogen isotope compositions of the natural gas in the gas reservoirs are generally heavy and have typical characteristics of high-maturity dry gas reservoirs. (2) The natural gas of the Feixianguan Formation is organic thermogenic gas, which is mainly oil-type gas generated by the secondary cracking of crude oil. The gas-generating parent material is mainly type II kerogen. (3) The natural gas of the Feixianguan Formation in the Eastern Sichuan Basin was mainly generated by argillaceous source rocks of the Upper Permian Longtan Formation. (4) Natural gas accumulation occurred as follows: the paleo-structure heights were filled with crude oil in the Early Jurassic, and paleo-oil reservoirs were formed in the Feixianguan Formation; during the Middle-Late Jurassic, the paleo-oil reservoirs were cracked when the reservoir temperatures rose above 160 °C, and paleo-gas reservoirs were formed. Since the end of the Late Jurassic, the paleo-gas reservoirs have been adjusted and reformed to form the present-day natural gas reservoirs. These results provide a basis for studying natural gas accumulation dynamics of the Feixianguan Formation in the Eastern Sichuan Basin.

© 2023 The Authors. Publishing services by Elsevier B.V. on behalf of KeAi Communications Co. Ltd. This is an open access article under the CC BY license (<http://creativecommons.org/licenses/by/4.0/>).

1. Introduction

World energy is entering a new stage of development with goals of low carbonization, diversification and cleanliness and is transforming from solid (wood and coal) and liquid (oil) to gaseous (natural gas) sources. In the new period of coping with global climate change and vigorously developing low-carbon energy, natural gas has become an insurmountable bridge for the transition

to clean energy and will play an irreplaceable role. Therefore, it is urgent to increase the intensity of natural gas exploration, promote technological innovation and integration, and strengthen basic research and continuous technological utilization of complex gas reservoirs.

Many oil and gas exploration practices show that known large and medium-sized gas fields are closely related to the distribution of source rocks. Oil and gas mainly accumulate around hydrocarbon kitchens, as indicated by the “source control theory” (Zuo et al., 2011; Pang et al., 2015; Luo et al., 2019; Yang et al., 2021). Therefore, it is of great significance to reveal the gas-source relationship and clarify the gas-source conditions when predicting natural gas

* Corresponding author.

E-mail address: zuoyinhui@tom.com (Y.-H. Zuo).

migration paths (Battani et al., 2000; Choi et al., 2013; Saadati et al., 2016; Song et al., 2022), exploring the distribution laws of petroleum systems (Magoon et al., 2005; Hao et al., 2009; Kotarba et al., 2014; Liu et al., 2021a), establishing accumulation models (Li Y et al., 2019; Li Q et al., 2020; Zheng et al., 2020; Song et al., 2022; Hu et al., 2022) and finding favorable exploration zones (Wu et al., 2020; Chen et al., 2021). In the 1980s, natural gas composition and carbon isotopes became important parameters for identifying natural gas origins, tracing gas sources and successfully guiding research on natural gas sources and favorable exploration zones (Schoell, 1980; Galimov, 1988). However, oil and gas exploration objects are expanding from conventional to unconventional, shallow to deep, and continental to sea areas, and gas-source conditions are becoming increasingly complex. The establishment of a new tracer index and a comprehensive geochemical tracer system has become an inevitable trend in natural gas source tracing. In recent years, indexes of hydrocarbon generation and accumulation tracers have been developed and improved continuously, such as hydrogen isotopes (Li Y et al., 2019; Li Q et al., 2020), biomarkers (Kotarba et al., 2014; Loomer et al., 2020; Ma et al., 2020; Spaak et al., 2020), and noble gas isotopes (Battani et al., 2000; Barry et al., 2018; Wang et al., 2019; Zheng et al., 2023). These indexes have been widely used in studies of hydrocarbon generation processes, oil and gas migration paths and oil and gas-source correlations of typical gas reservoirs, which provide an important theoretical basis and technical support for oil and gas exploration (Wang et al., 2019; Li et al., 2020; Loomer et al., 2020).

In the early 1960s, the industrial flow of gas from Well Ba 3 was established in the Shiyogou structure of the Eastern Sichuan Basin (ESB), and a prelude to oil and gas exploration was opened in the Lower Triassic Feixianguan Formation. Thereafter, gas reservoirs of the Feixianguan Formation were discovered in several structures, such as the Luojiashai, Puguang, Tieshanpo, Dukouhe and Jinzhuping structures. As of 2015, the number of explored reserves reached $1.87603 \times 10^{11} \text{ m}^3$, which indicated good exploration prospects for the region. However, geochemical parameters such as natural gas composition and carbon isotopes lose their original significance as indicators of the Feixianguan Formation in the ESB, mainly due to the development of H_2S -rich gas reservoirs that were subjected to secondary alteration of the TSR (thermochemical sulfate reduction) reaction in later stages (Cai et al., 2013; Hu et al., 2014; Liu et al., 2019), the complex geological conditions of oil and gas, extensive natural gas evolution and multisource and multistage accumulation (Hu et al., 2014; Liu et al., 2019). Therefore, it is more difficult to study the origins and main sources of natural gas in the study area, which restricts studies of natural gas accumulation dynamics in the Feixianguan Formation and leads to low success rates for natural gas explorations in the region. Through investigation, it is found that there were still controversies about the gas source in the study area, mainly including three viewpoints. Based on a small amount of natural gas composition, carbon isotope and biomarker data, the source rocks of the Upper Permian Longtan Formation are considered the main source rocks (Ma, 2008; Zhao et al., 2011; Li et al., 2016; Wu et al., 2019). Through natural gas composition and stable isotope studies, it was concluded that the Upper Permian Longtan Formation and Silurian source rocks have made certain contributions to the natural gas of the Feixianguan Formation (Hu et al., 2014; Liu et al., 2014). Based on some natural gas components and biomarker data, the carbonate rocks of the Changxing Formation and argillaceous source rocks of the Longtan Formation are considered to be the main source rocks (Yang et al., 2002). The main reasons for this divergence are limited geochemical data and the lack of research methods, without considering the multiplicity of a single geochemical index and the complexity of geological conditions in the study area. In addition, the research on

the characteristics of source rocks is limited, which cannot effectively establish the source-reservoir relationship. In view of the controversial issues surrounding the gas source of the Lower Triassic Feixianguan Formation, geochemical experimental analysis of the natural gas, source rocks and reservoir asphalts was carried out. Sixty-nine natural gas composition data, 42 carbon isotope data, 29 hydrogen isotope data, 9 noble gas isotope data, 49 biomarker data and 23 family component carbon isotope data were obtained. On this basis, the geochemical characteristics, natural gas origin and gas-source correlation of the Lower Triassic Feixianguan Formation in the ESB were studied. Then, a model for the accumulation of the Feixianguan Formation in this area was established to provide guidance for further research on gas accumulation dynamics and exploration deployment.

2. Geological settings

The Sichuan Basin is a typical marine-continental sedimentary multicycle superimposed basin, which is located on the eastern side of the Qinghai-Tibet Plateau and the northwestern margin of the Yangtze Plate in the geological structure (Liu et al., 2021b). The basin is surrounded by high mountains, the Micang Mountains-Daba Mountains in the north, Daliangshan Mountain and Lou Mountain in the south, Longmen Mountain and Qionglai Mountain in the west, and Qiyue Mountain in the east. The whole basin has a rhombic distribution and shows multi-structural boundaries and multi-structural systems controlled by deep, large faults. Bounded by large-scale faults, the basin can be divided into six tectonic units, namely, the North Sichuan low-flat structure, Western Sichuan low-steep structure, Central Sichuan low-flat structure, Southwest Sichuan low-gentle structure, Eastern Sichuan high-steep structure (referred to as the ESB) and Southern Sichuan low-steep structural area (Fig. 1a) (Cai, 2016).

The ESB is located east of Huaying Mountain, west of Qiyue Mountain, south of Daba Mountain and north of the Chongqing-Qijiang River, and it exhibits an area of approximately $2.7 \times 10^4 \text{ km}^2$ (Fig. 1b). The ESB has multiple steep anticline belts, such as the Huaying and Qiyue Mountains, which are generally characterized by closed anticlines and open synclines, i.e., ejective folds. The Sichuan Basin has experienced multistage structural movements, such as the Jinning Movement, Caledonian Movement, Indosinian Movement, Yanshan Movement and Himalayan Movement, which have resulted in complex structures. As indicated by these tectonic movements, basin tectonic evolution can be divided into three stages (Liu et al., 2015, 2021b): (1) a marine carbonate platform from the Late Sinian to the Middle Triassic; (2) foreland basins from the Late Triassic to the Late Cretaceous; and (3) a denudation and structural adjustment stage in the Cenozoic. More than 10,000 m of strata were developed in the ESB from the Sinian to Quaternary. The Sinian-Middle Triassic was dominated by marine carbonate strata, and the strata above the Middle Triassic are continental clastic (Fig. 1c) (Liu et al., 2020). Controlled by rift troughs and sedimentary depressions, six sets of high-quality source rocks were developed vertically in the study area. Among them, the underlying potential gas-source rocks of the Feixianguan Formation mainly include the argillaceous source rocks of the Silurian Longmaxi and the Upper Permian Longtan Formations (including the Wujiaping Formation with simultaneous heterogeneity) and the carbonate source rocks of the Changxing Formation (Table 1).

3. Samples and methods

Based on the principle of well location dispersion and drilling and logging data, 69 representative natural gas samples and 11

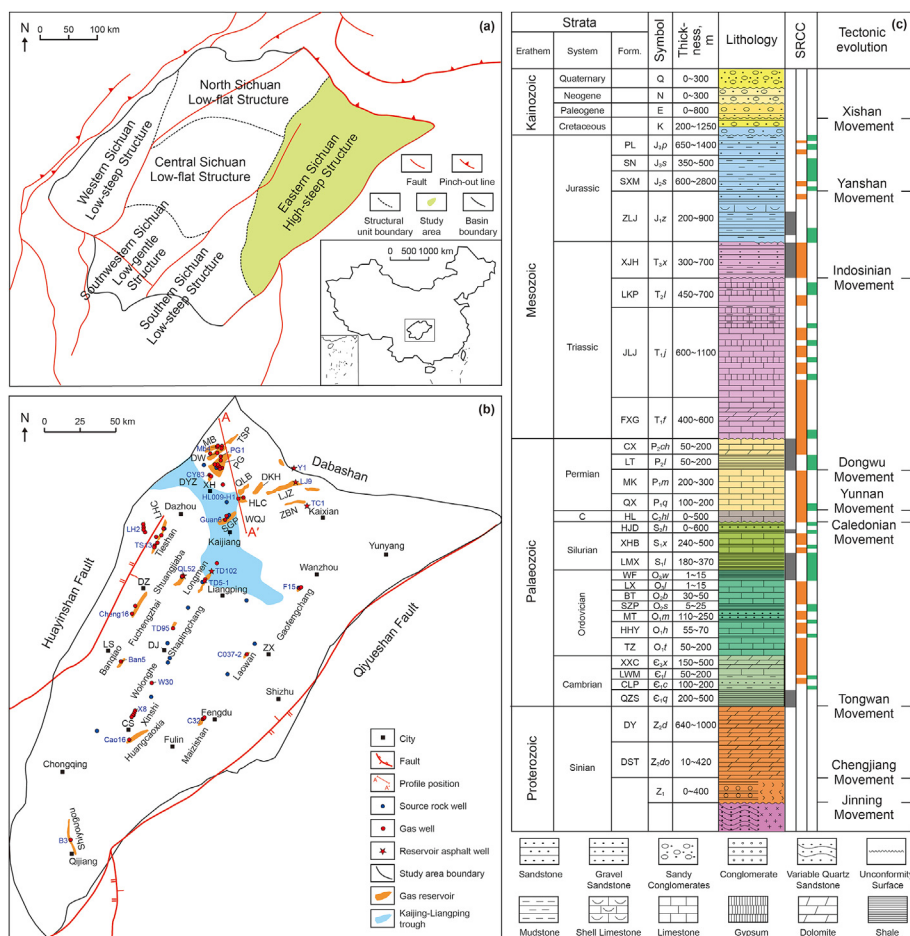


Fig. 1. (a) Tectonic zoning of the Sichuan Basin (Cai, 2016). (b) The distribution of gas reservoirs and wells in the Feixianguan Formation in the Eastern Sichuan Basin. (c) Stratigraphic column section of the Eastern Sichuan Basin (based on Liu et al., 2020). MB = Maoba; TSP = Tieshanpo; PG = Puguang; QLB = Qilibei; DKH = Dukouhe; LJZ = Luoqiazhai; DW = Dawan; DYZ = Dongyuezhai; ZBN = Zhengbanan; LHC = Longhuichang; SGP = Shaguanping; HLC = Huanglongchang; WQJ = Wenqianjiang; DZ = Dazhu; ZX = Zhongxian; DJ = Dianjiang; LS = Linshui; CS = Changshou; XH = Xuanhan; C = Carboniferous; PL = Penglai Formation; SN = Suining Formation; SXM = Shaximiao Formation; ZLJ = Ziliujing Formation; XJH = Xujiaba Formation; LKP = Leikoupo Formation; JLJ = Jialingjiang Formation; FXG = Feixianguan Formation; CX = Changxing Formation; LT = Longtan Formation; MK = Maokou Formation; QX = Qixia Formation; HL = Huanglong Formation; HJD = Hanjiadian Formation; XHB = Xiaheba Formation; LMX = Longmaxi Formation; WF = Wufeng Formation; LX = Linxiang Formation; BT = Baota Formation; SZP = Shizipu Formation; MT = Meitan Formation; HHY = Honghuayuan Formation; TZ = Tongzi Formation; XXC = Xixiangchi Formation; LWM = Longwangmiao Formation; CLP = Canglangpu Formation; QZS = Qiongzhusi Formation; DY = Dengying Formation; DST = Doushantuo Formation; SRCC = source-reservoir-cap combination.

Table 1
Geochemical characteristics of potential gas-source rocks in the Feixianguan Formation, Eastern Sichuan Basin (Ma, 2008).

Formation	Lithology	Thickness, m	TOC, wt %	R ₀ , %	Organic matter type	Comprehensive evaluation
Changxing	Carbonate rock	0–380	0.15–1.50	>2.0	I–II type	Poor-medium
Longtan	Dark mudstone	20–120	1.20–7.80	1.5–2.8	mainly II type	Good
Longmaxi	Dark mudstone	150–800	0.30–2.10	2.4–3.7	mainly I–II type	Good

TOC = Total organic carbon; R₀ = Vitrinite reflectance.

reservoir solid asphalt samples were collected in the typical gas reservoirs in the Lower Triassic Feixianguan Formation, and 38 source rock samples were collected in the typical structures in the Upper Permian Changxing and Longtan Formations. To minimize the impact of air pollution and sampling on data measurement, strict processing measures were needed during natural gas sampling: (1) A high-pressure steel cylinder with double valves and an anti-H₂S corrosion-resistant coating was selected for sampling. (2) Vacuum equipment was used to pre-pump the sampling cylinder before sampling, and the vacuum level was at least 10⁻³ Pa. (3) The cylinder was repeatedly washed 4–6 times with natural gas in the high-pressure wellhead during sampling and finally sampled in the middle part of the continuous gas flow.

The natural gas samples were tested for natural gas composition, hydrocarbon isotope composition and noble gas isotopes. The source rocks and reservoir asphalt samples were tested for chloroform bitumen “A” and group component carbon isotopes and GC/MS studies for saturated hydrocarbons. The tests were completed in the Key Laboratory of Natural Gas Accumulation and Development, China Petroleum Exploration and Development Institute.

- (1) Natural gas components were analyzed with a SCION 456-GC gas chromatograph (Original manufacturer: Tianmei Yituo, USA), with high-purity helium as the carrier gas, and tested with a double TCD detector. The carbon and hydrogen isotopes of the natural gas were tested on a Finnigan MAT-252

MS (Original manufacturer: Finnigan Mat, Germany). The carbon and hydrogen contents of each component were calibrated to the international standard (VPDB and V-SMOW, respectively), and the standard deviation was 3‰.

- (2) The noble gas isotope test standard was SY/T 7359–2017 (Oil and gas industry standards of the People's Republic of China); the experimental environment was room temperature 20–25 °C and relative humidity < 70%. The experimental process was divided into the following steps. First, the natural gas cylinder was connected to the device injection port through a pressure reducing valve, and the mechanical pump, molecular pump and ion pump were used to evacuate the system. Second, the zirconium-based furnace was heated to 690 °C for 30 min and then cooled to 350 °C. Third, the injection volume of natural gas samples was controlled by an injection control valve and vacuum gauge. Fourth, the active gas in natural gas samples was purified with a zirconium-based furnace and then enriched with rare gas. Fifth, liquid nitrogen was used to separate the He, Ne, Ar, Kr and Xe components based on the different boiling points of these rare gases. Finally, He and Ar were successively sent to a rare gas isotope mass spectrometer in a static vacuum for isotope analysis.
- (3) The experimental environment for GC/MS studies of the saturated hydrocarbons was: a temperature of 25 °C and relative humidity of 57%. The experimental process was divided into the following steps. First, the surfaces of the samples were polluted and crushed to 0.125 mm. Then, the carbon isotopes of the sample extracts were analyzed after Soxhlet extraction (chloroform) for 72 h. Second, asphaltene was separated with n-hexane. Saturated hydrocarbons, aromatic hydrocarbons and nonhydrocarbon components were separated successively with a silica gel alumina chromatography column and solvents of different polarities. Third, the carbon isotopes of each group of components were tested. Finally, the saturated hydrocarbons were analyzed by an Agilent 6890N GC (Original manufacturer: Agilent Company, USA) and an Agilent 5977A GC-MS (Original manufacturer: Agilent Company, USA). The conditions for GC/MS were as follows: the carrier gas was high-purity helium with a flow rate of 1 mL/min. An HP-5MS (60 m × 0.25 mm × 0.25 μm) column was used with an EI source. The temperature was increased from 100 °C to 120 °C at a rate of 10 °C/min, to 250 °C at a rate of 4 °C/min, then to 300 °C at a rate of 1 °C/min, and held for 40 min.

4. Experimental results

4.1. Geochemical characteristics of natural gas

4.1.1. Characteristics of natural gas compositions

There were great differences in the relative contents of natural gas components in different gas reservoirs of the Feixianguan Formation in the ESB (Table S1). According to the classification scheme for H₂S gas reservoirs developed by Dai (1985), the gas reservoirs of the Feixianguan Formation in the study area were divided into two categories: H₂S-rich gas reservoirs (H₂S content greater than 2%) and H₂S-poor gas reservoirs (H₂S content less than 2%).

The H₂S-rich gas reservoirs are widely distributed east of the Kaijiang-Liangping trough. The methane content in the hydrocarbon gas ranged from 71.160% to 92.417%, with an average of 79.225%. The ethane content ranged from 0.020% to 0.215%, with an average of 0.057% (Fig. 2a). The heavy hydrocarbon contents of

propane and above were almost undetectable. The drying coefficient of natural gas was greater than 99.700%, with an average of 99.882%, which indicated that it belongs to a typical dry gas reservoir (Fig. 2b). The content of nonhydrocarbon gases was high and mainly included H₂S and CO₂, in which the content of CO₂ was between 0.460% and 18.030%, with an average of 7.633% (Fig. 2d). The H₂S content ranged from 2.020% to 17.760%, with an average of 11.896% (Fig. 2d). In addition, the nonhydrocarbon gases contained small amounts of N₂, He, and H₂ (Fig. 2c).

The H₂S-poor gas reservoirs are mainly distributed west of the Kaijiang-Liangping trough and the shelf area. Natural gas is dominated by hydrocarbon gases. Among them, the methane content was 88.926%–99.320%, with an average of 97.491%, the ethane content was 0–3.130%, with an average of 0.429% (Fig. 2a), and the heavy hydrocarbon contents of propane and above were very low. The drying coefficient of natural gas was mostly above 99.000%, with an average of 99.428%, indicating that the gas reservoir was a dry gas reservoir with a high degree of thermal evolution (Fig. 2b). Nonhydrocarbon gases were mainly H₂S, N₂, CO₂ and small amounts of He and H₂, in which the H₂S content was between 0–0.590%, with an average of 0.113%, and the CO₂ content was between 0–5.700%, with an average of 0.425% (Fig. 2c and d).

4.1.2. Characteristics of carbon isotopes

The natural gas of the Feixianguan Formation in the ESB was dry gas, and most samples had little propane content. Therefore, only the carbon isotopes of methane and ethane could generally be measured, and only methane could be measured in some samples (Table S1). The results showed that the distribution of δ¹³C₁ values for natural gas in the Feixianguan Formation was relatively concentrated (Fig. 3a), and there was no significant difference between H₂S-rich gas reservoirs and H₂S-poor gas reservoirs. The δ¹³C₁ values of H₂S-rich gas reservoirs were between –33.50‰ and –28.90‰ and were mainly distributed between –32‰ and –29‰. The δ¹³C₁ values of H₂S-poor gas reservoirs were between –33.80‰ and –28.63‰ and were mainly distributed between –33‰ and –30‰. The distribution of δ¹³C₂ values was relatively wide (Fig. 3b). The δ¹³C₂ values of the H₂S-rich gas reservoir were –32.40‰––26.81‰, with an average of –28.94‰, and those of the H₂S-poor gas reservoirs were –37.00‰––26.93‰, with an average of –33.44‰. There was a significant difference between the two gas reservoirs.

4.1.3. Characteristics of hydrogen isotopes

Analyses of 37 hydrogen isotope samples from the study area showed that the distributions of δD₁ values for natural gas in H₂S-rich gas reservoirs and H₂S-poor gas reservoirs were relatively concentrated and generally heavy. There were no significant differences between them (Table S1 and Fig. 4a). The δD₁ values ranged from –147.00‰ to –115.00‰ and were mainly distributed between –140.00‰ and –130.00‰ with an average of –132.43‰. This result indicated that the extent of thermal evolution in the natural gas in the Feixianguan Formation in the ESB was high, and the sedimentary environment was relatively simple. The distribution of δD₂ values was relatively wide (Fig. 4b). The δD₂ values of H₂S-rich gas reservoirs were between –137.61‰ and –115.02‰ and mainly between –120.00‰ and –110.00‰ with an average of –123.23‰. The δD₂ values of H₂S-poor gas reservoirs were between –170.00‰ and –118.00‰ and mainly between –150.00‰ and –130.00‰ with an average of –137.49‰. There were obvious differences between them.

4.1.4. Characteristics of noble gas isotopes

In this study, nine natural gas samples from the Feixianguan Formation in the ESB were tested and the noble gas isotopes were

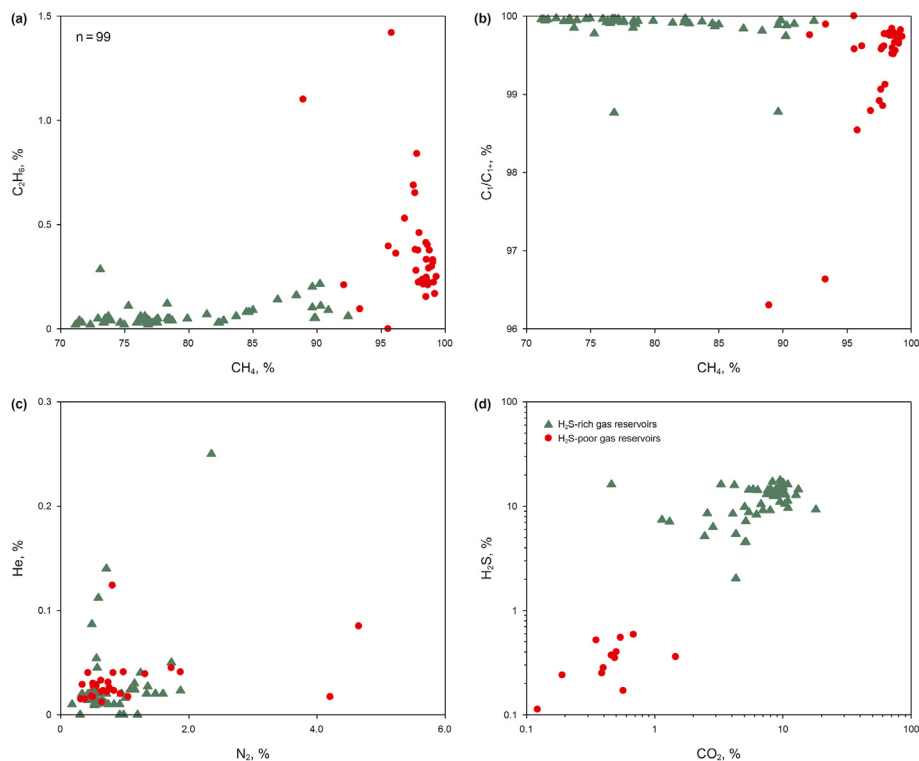


Fig. 2. Natural gas characteristics of the Feixianguan Formation, Eastern Sichuan Basin (some data comes from Yang et al., 2002; Zhang et al., 2007; Hu, 2009; Zhang et al., 2018) (a) Relationship between methane and ethane content. (b) Relationship between drying coefficient and methane content. (c) Relationship between CO_2 and H_2S content. (d) Relationship between CO_2 and H_2S content.

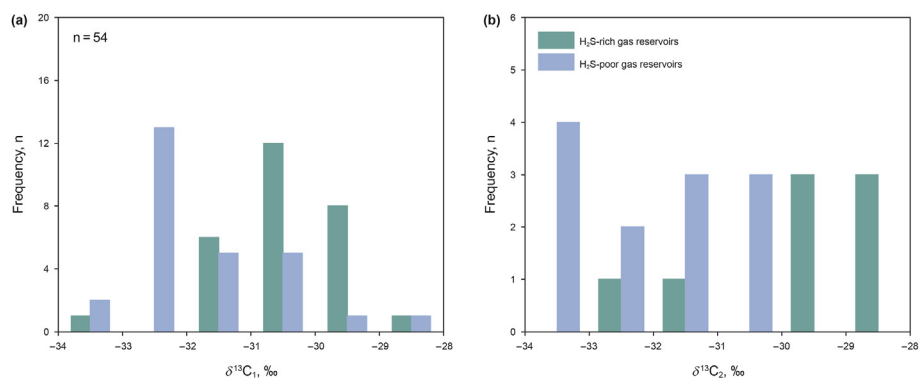


Fig. 3. Carbon isotope characteristics of natural gas in the Feixianguan Formation, Eastern Sichuan Basin (a) Carbon isotopes of methane. (b) Carbon isotopes of ethane.

analyzed. The $^3\text{He}/^4\text{He}$ value of He is $(4.303\text{--}8.469) \times 10^{-8}$, with an average of 6.274×10^{-8} . The $^{40}\text{Ar}/^{36}\text{Ar}$ values of Ar vary widely and range from 315.738 to 974.753 with an average of 636.117. The $^3\text{He}/^4\text{He}$ values of natural gas fall in the typical crustal source genetic region (Table 2 and Fig. 5), indicating that noble gases in the natural gas of the Feixianguan Formation gas reservoirs belong to the typical crustal source origin region. This also showed that the tectonic movements in the study area are relatively stable, and there is a lack of deep faults that communicate with the mantle.

4.2. Geochemical characteristics of reservoir asphalt

The distributions of n-alkanes were generally complete in the asphalt samples of the Feixianguan Formation reservoirs in the ESB, and the carbon numbers were $\text{nC}_{12}\text{--nC}_{34}$. There was no

obvious “drum package” (“UCM”, Unresolved Complex Mixture) in the baseline for alkane chromatography, indicating that there was no significant biodegradation (Fig. 6). The distribution of n-alkanes generally showed a “single peak and post-peak” with the main carbon peak near nC_{24} . The $\Sigma\text{nC}_{21}\text{--}/\Sigma\text{nC}_{22+}$ value was 0.01–1.43, with an average value of 0.22. The Pr/Ph value was 0.37–0.67, with an average of 0.54. The pr/ nC_{17} was 0–0.67, with an average of 0.45. The Ph/ nC_{18} ranged from 0 to 0.83, with an average of 0.45. The $\text{C}_{35}\text{H}\text{--}22\text{S}/\text{C}_{34}\text{H}\text{--}22\text{S}$ values were 0.43–0.81, with an average of 0.57. Ts/(Ts + Tm) ranged from 0.31 to 0.53, with an average of 0.44. The gammacerane index (Ga/ C_{30}H) was 0.06–0.36, with an average of 0.21 (Table S2). The distribution of $\alpha\alpha\alpha 20\text{R}\text{--}\text{C}_{27}$, C_{28} and C_{29} regular steranes was the “V” type, and the C_{29} regular sterane proportion was slightly larger than the C_{27} regular sterane proportion (Fig. 6).

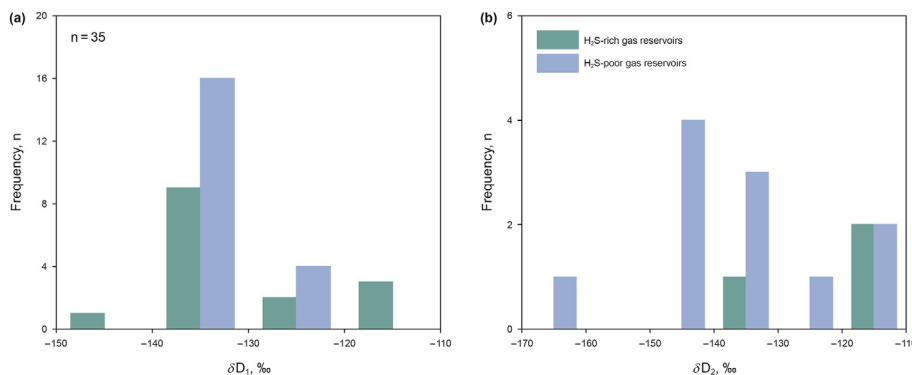


Fig. 4. Hydrogen isotope characteristics of natural gas in the Feixianguan Formation, Eastern Sichuan Basin (a) Hydrogen isotopes of methane. (b) Hydrogen isotopes of Ethane.

Table 2
Characteristics of the noble gas isotope in the Feixianguan Formation, Eastern Sichuan Basin.

Well	³ He/ ⁴ He, 10 ⁻⁸	Relative error, 10 ⁻⁸	⁴⁰ Ar/ ³⁶ Ar	Relative error	Calculation of geological age, Ma ^A	Calculation of geological age, Ma ^B
TS13	4.75	±0.181	316	±1	3.54	241.78
TS1	5.112	±0.174	397	±1	56.16	255.06
LH6	7.165	±0.289	490	±2	104.77	242.07
HL009-H1	4.303	±0.259	975	±5	263.41	263.41
Cheng16	4.799	±0.159	926	±3	251.59	251.59
TD5-1	7.184	±0.560	780	±3	212.04	259.96
C037-2	8.469	±0.268	387	±1	50.44	253.46
X8	7.243	±0.289	760	±3	205.91	258.13
Ban5	7.437	±0.375	695	±1	185.55	252.37

A = The calculation result from Formula (1); B = The calculation result from Formula (2).

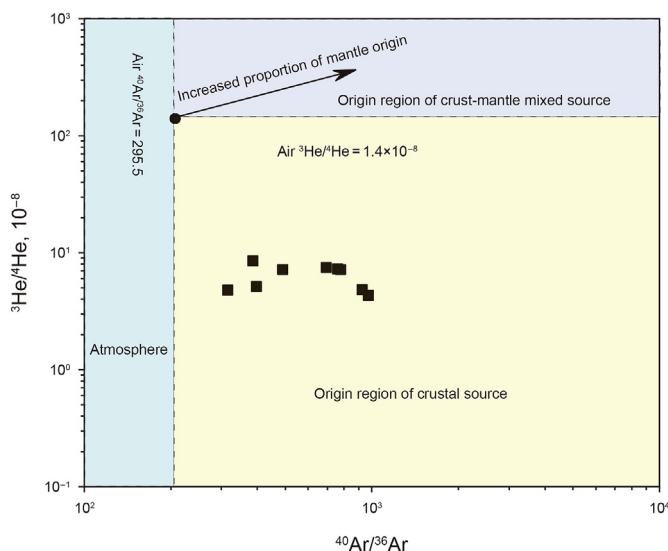


Fig. 5. Relationship between ⁴⁰Ar/³⁶Ar-³He/⁴He of natural gas in the Feixianguan Formation, Eastern Sichuan Basin (based on Wang et al., 2019).

The carbon isotopes of soluble extracts and their group components in reservoir asphalt were generally light. The δ¹³C of chloroform asphalt “A” was between -29.9‰ and -29.4‰. The δ¹³C of saturated hydrocarbons ranged from -29.5‰ to -30.0‰. The δ¹³C of aromatic hydrocarbons ranged from -29.5‰ to -28.9‰. The δ¹³C of nonhydrocarbon ranged from -29.7‰ to -28.6‰. The δ¹³C of asphaltene ranged from -28.4‰ to -27.9‰ (Table 3).

5. Discussion

5.1. Origin of natural gas

The H₂S in the Feixianguan Formation gas reservoirs belonged to TSR origin in the ESB (Cai et al., 2013; Liu et al., 2019). TSR is the reaction of hydrocarbons and sulfates in a specific environment driven by thermal power. With oxidation and alteration of hydrocarbons, the drying coefficient of the natural gas increases, and the stable isotope weight of heavy hydrocarbon gas increases (Liu et al., 2019). This study showed that the TSR reaction gradually decreased with decreasing hydrocarbon carbon number, so the influence of the TSR reaction on methane carbon and hydrogen isotopes was relatively small (Liu et al., 2014; Wu et al., 2016). Therefore, the natural gas geochemical data for H₂S-poor gas reservoirs (natural gas composition and ethane carbon isotope) and the stable isotope of natural gas methane in the study area were used only to identify the origin of natural gas.

There are certain differences in hydrocarbon components between kerogen-cracked gas and oil-cracked gas. Therefore, the identification charts of the ln (C₁/C₂) and ln (C₂/C₃) established by predecessors, which consider thermal evolution (Prinzhofer and Huc, 1995; Xie et al., 2016), can be used to identify them. The ln (C₁/C₂) of the natural gas in the Feixianguan Formation of the ESB was basically unchanged, and the ln (C₂/C₃) changed greatly, indicating that it is oil-cracked gas with high maturity (Fig. 7a).

The carbon isotope value is less affected by the secondary effects of reservoir formation, and it can be used to determine the origin of the natural gas. On the “Bernard” diagram (Bernard et al., 1976), the natural gas of the Feixianguan Formation was mainly distributed in the thermogenic gas area, and the gas-generating parent material was mainly type II kerogen (Fig. 7b). In addition, ethane carbon

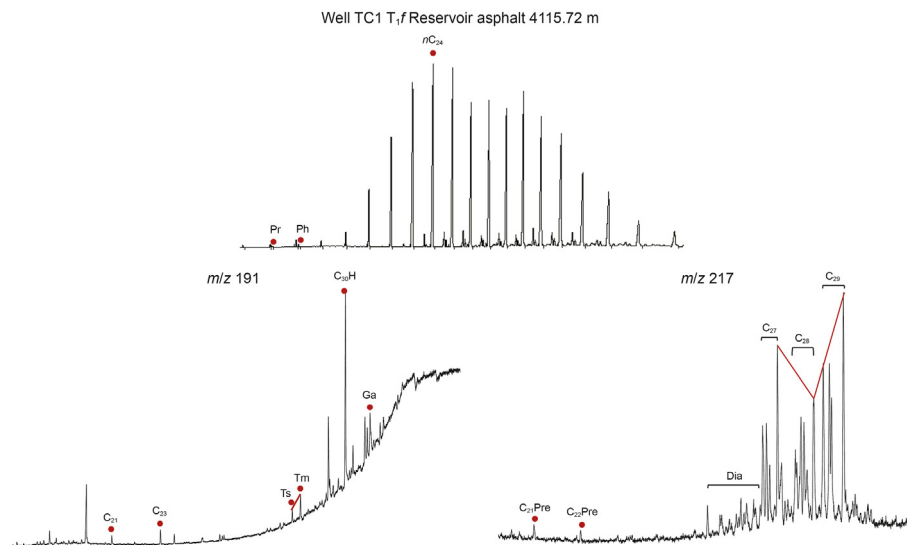


Fig. 6. Saturated hydrocarbon GC and GC/MC diagram of reservoir asphalt in the Feixianguan Formation, Eastern Sichuan Basin
 Ts: C₂₇ 18 α (H)-22, 29, 30-trisnorneohopane; Tm: C₂₇ 17 α (H)-22, 29, 30-trisnorhopane; Ga = Gammacerane; Pre = Progesterone; Dia = Rearranged sterane; H = Hopanes.

Table 3
 Characteristics of carbon isotopes of the reservoir asphalts chloroform asphalt “A” and group components in the Feixianguan Formation and Upper Permian source rocks, Eastern Sichuan Basin.

Well no.	Depth, m	Formation	$\delta^{13}C$, ‰				
			Chloroform asphalt “A”	Saturated hydrocarbons	Aromatic hydrocarbons	Nonhydrocarbons	Asphaltenes
TC1	4115.4	Feixianguan	-29.40	-29.50	-28.90	-28.60	-27.90
TD102	3847.8	Feixianguan	-29.90	-30.00	-29.50	-28.40	-28.40
TS101-X2	3661.0	Longtan	-29.40	-30.00	-28.70	-29.20	-28.50
TD004-X3	4275.0	Longtan	-28.40	-29.00	-28.10	-28.70	-28.60
TD004-X3	4338.0	Longtan	-28.70	-29.30	-28.20	-28.70	-28.40
F007-H3	4558.0	Longtan	-28.10	-29.30	-28.30	-28.70	-28.30
BJ001-H1	3962.0	Longtan	-28.50	-29.50	-29.00	-28.80	-27.90
BJ001-H1	4005.0	Longtan	-29.10	-29.60	-29.40	-29.60	-28.40
Guan008-X1	4088.0	Longtan	-28.20	-29.50	-28.80	-27.60	-28.20
Guan008-X1	4130.0	Longtan	-28.40	-29.50	-28.60	-27.70	-27.80
WQ002-H4	4221.0	Longtan	-29.30	-29.90	-28.40	-28.70	-27.90
TX5	3872.0	Longtan	-29.80	-30.50	-29.50	-29.50	-28.50
TX5	3918.0	Longtan	-29.30	-29.60	-29.00	-29.10	-28.40
QL017-X1	4373.0	Longtan	-29.10	-30.20	-29.30	-28.20	-26.60
YA006-X5	4460.0	Longtan	-28.50	-29.60	-28.70	-29.00	-27.90
YA006-X5	4511.0	Longtan	-28.90	-29.50	-28.60	-28.90	-27.80
YA006-X5	4593.0	Longtan	-28.90	-29.60	-28.60	-28.70	-28.40
YA006-X5	4614.0	Longtan	-28.80	-29.60	-28.90	-29.10	-28.00
GX003-H1	4042.0	Longtan	-28.70	-29.50	-28.50	-28.40	-28.40
TD81	4472.0	Longtan	-28.90	-29.50	-29.30	-29.10	-28.10
PG5	5157.0	Changxing	/	-29.58	-25.50	-26.81	-24.93
PG5	5167.0	Changxing	/	-29.24	-27.91	-27.01	/
XQX3	5163.0	Changxing	/	-29.03	-26.87	-27.39	-26.68

isotopes showed strong primary parent material inheritance, and natural gas generated by different types of organic matter shows different trends in the correlation diagram of methane and ethane carbon isotopes (Liu et al., 2012). Most natural gas samples of the Feixianguan Formation in the ESB were distributed near type II kerogen in the Delaware/Val Verde Basin (Rooney et al., 1995), reflecting that the gas-generating parent material was mainly type II kerogen in the Feixianguan Formation in the study area (Fig. 7c). A combination of carbon isotopes and hydrogen isotopes can provide important information on the genesis of natural gas and the sedimentary environment of the hydrocarbon-generating parent material (Schoell, 1980). The diagram shows that the gas-generating parent material was a mainly transitional organic matter in the Feixianguan Formation, followed by sapropelic organic

matter, and indicated a sedimentary environment of saline-brackish water (Fig. 7d).

5.2. Gas source comparison

5.2.1. Gas–gas comparison

The ethane carbon isotope exhibited strong maternal inheritance, which is of special significance in a study of gas-source correlation. By comparing the carbon isotopes of the Feixianguan Formation, Jialingjiang Formation, Changxing Formation and Carboniferous Formation gas reservoirs in the ESB, it was found that the $\delta^{13}C_1$ values for each production layer were concentrated in the range -34‰–30‰ (Fig. 8a), which showed that the thermal evolution of each production layer was high. The $\delta^{13}C_2$ values of

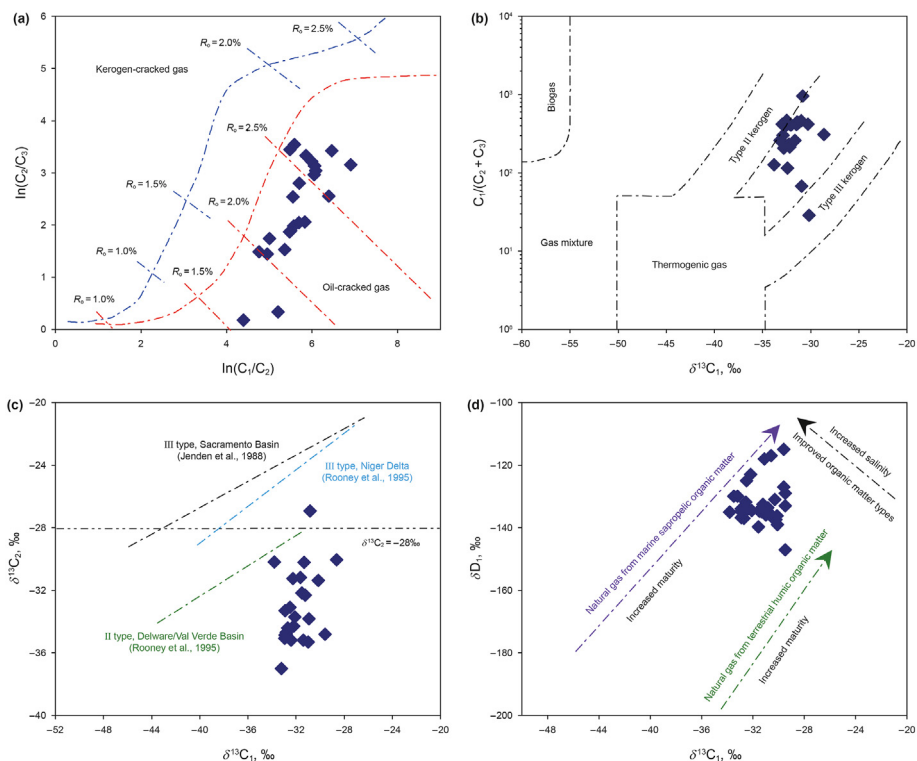


Fig. 7. Genetic identification of natural gas in the Feixianguan Formation, Eastern Sichuan Basin (a) Correlation diagram of $\ln(C_1/C_2)$ - $\ln(C_2/C_3)$ (based on Xie et al., 2016). (b) Correlation diagram of $\delta^{13}C_1$ and $C_1/(C_2+C_3)$ (based on Bernard et al., 1976). (c) Correlation diagram between $\delta^{13}C_1$ and $\delta^{13}C_2$ (Sacramento basin from Jenden et al., 1988; Delaware/Val Verde basin from Rooney et al., 1995; Niger Delta Basin from Rooney et al., 1995). (d) Correlation diagram of $\delta^{13}C_1$ and δD_1 (based on Schoell, 1980).

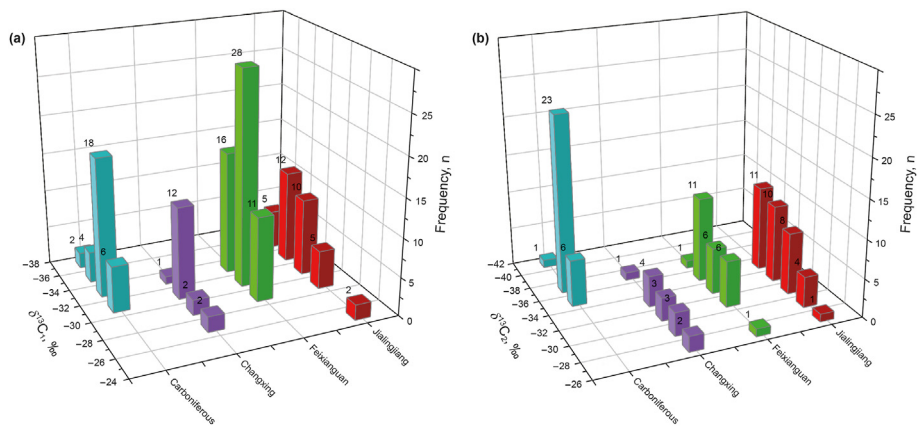


Fig. 8. Comparison of carbon isotopes of natural gas in different layers in the Eastern Sichuan Basin (a) Carbon isotopes of methane. (b) Carbon isotopes of ethane

natural gas in the Feixianguan Formation after removing the TSR were similar to those in the Jialingjiang Formation and Changxing Formation. The $\delta^{13}C_2$ values were mainly distributed between -36% and -30% , which meant that they have homology (Fig. 8b). The $\delta^{13}C_2$ values of natural gas in the Carboniferous were generally lighter and ranged primarily from -38% to -36% . There were obvious differences between natural gases from the two strata and different sources.

5.2.2. Reservoir asphalt-source rock correlation

The dry coefficient of natural gas was generally high for the Feixianguan Formation of the ESB. The carbon isotopes of methane

and ethane are most commonly for generating gas-source correlations in this area, and a comparison of heavy hydrocarbon carbon isotopes and light hydrocarbon compounds cannot be carried out, which seriously restricts the study of gas-source correlation in the ESB. The natural gas of the Feixianguan Formation in the study area is crude oil cracking gas, and a large amount of asphalt is developed in the reservoir (Ma, 2008), which was the product of thermal cracking of paleo-oil reservoirs. It records geological and geochemical information in the evolutionary history of crude oil after the formation of the oil reservoirs and is an important means with which to clarify natural gas sources with high overmaturity.

The contents of sterane compounds decrease during high

maturity evolution, but the distribution of $\alpha\alpha\alpha 20R-C_{27}$, C_{28} and C_{29} regular steranes are not significantly affected (Lu et al., 2017). Therefore, $\alpha\alpha\alpha 20R-C_{27}$, C_{28} and C_{29} regular steranes can be used as reliable indicators of gas-source correlations with high over-maturity. It is generally believed that C_{27} sterane is mainly related to lower hydrobionts and algae organic matter, and C_{29} sterane can indicate a higher plant origin (Huang and Meinschein, 1979).

Comparisons showed that the distribution characteristics of regular steranes in the asphalt samples of the Feixianguan Formation reservoirs were closely related to the hydrocarbon source rocks of the Longtan Formation. Both contain abundant $\alpha\alpha\alpha 20R-C_{27}$, C_{28} and C_{29} regular steranes with a “V” shaped distribution, and the C_{29} regular sterane proportion was slightly larger than the C_{27} regular sterane proportion (Table S2). This indicated that the oil-generating parent materials had the characteristics of mixed inputs from phytoplankton and higher plants, which is consistent with the sedimentary environment of the marine-land interactions of the Longtan Formation. The source rocks of the Changxing Formation and Silurian Longmaxi Formation showed the characteristics of mixed input from phytoplankton, bacteria and algae, which were dominated by contributions from phytoplankton and bacteria. They showed a significantly poor affinity with the Feixianguan Formation reservoir asphalt (Fig. 9).

The carbon isotope composition of solid asphalt reflects the inheritance of the organic carbon isotope composition of the source rock, and later secondary changes have little effect on it. Due to the influence of isotope fractionation, the carbon isotopes of reservoir asphalt and its group components with high overmaturity are generally close to or higher than that of source rock kerogen at 1‰–2‰ (Machel et al., 1995), which provides reliable parameters for studies of gas-source correlations in the study area. In this study, the $\delta^{13}C$ curve of the extract and its group components was generally light in the source rock of the Longtan Formation (Table 3), which is in good agreement with the reservoir asphalt of the Feixianguan Formation. However, that of the source rock in the Changxing Formation was relatively heavy and had a poor affinity (Fig. 10). The above analysis shows that the reservoir asphalt of the

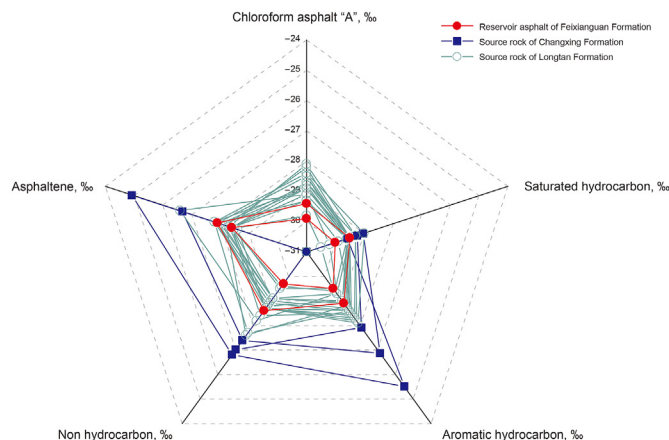


Fig. 10. Comparison of the carbon isotope of extract and its group components between reservoir asphalts of the Feixianguan Formation, Eastern Sichuan Basin and source rocks of Upper Permian.

Feixianguan Formation mainly came from the Longtan Formation source rock in the study area.

5.2.3. Noble gas chronology

For quantitative calculations of natural gas-source rock ages, hydrogen isotope compositions are more accurate than helium isotope compositions. According to the relationship between the $^{40}Ar/^{36}Ar$ value of natural gas and the source rock age proposed by Liu and Xu (1993):

$$T = 530 \times \lg(^{40}Ar/^{36}Ar) - 1323 \tag{1}$$

where T is the stratum age of the source rock, Ma, and $^{40}Ar/^{36}Ar$ is the $^{40}Ar/^{36}Ar$ value of the natural gas.

Except for the geological ages calculated by natural gas in Well HL 009-H1 and Well Cheng 16 (263.41 Ma, 251.59 Ma), the calculated ages were relatively consistent with the geological ages of the Longtan Formation (256–240 Ma) (Cai, 2016; Liu et al., 2020). However, the ages of source rocks calculated with other samples were mainly from Jurassic to Quaternary, which was obviously inconsistent with the development characteristics of actual source rocks in the study area. Through analysis, it was considered that the formula proposed by Liu and Xu (1993) for calculating the source rock age was obtained for conditions in which the parent source rock was mudstone. The study shows that the $^{40}Ar/^{36}Ar$ ratio of natural gas has an obvious linear relationship with the potassium content in the source rock when the gas source is of the same age. The coal measure strata were developed in the central and southern parts of the study area (Zhu et al., 2012). The potassium content of the parent element from radiogenic ^{40}Ar in the strata was much lower than that in mudstone, which led to the low ^{40}Ar proportion in the source rock. The $^{40}Ar/^{36}Ar$ values of natural gas were significantly lower in Well LH 6, Well Xin 8, Well Ban 5 and Well TD 5–1 in the southern part of the ESB. It is worth noting that previous studies confirmed that the natural gas of the Feixianguan Formation was oil-cracked gas in the ESB, which excluded a contribution from coal rock to the gas reservoirs of the Feixianguan Formation. Therefore, the study in this paper further explains the obvious difference in potassium contents between carbonaceous mudstone and mudstone.

According to the potassium contents in coal measure strata (0.2%–0.6%) (Liu and Xu, 1993) and the linear correlation between the $^{40}Ar/^{36}Ar$ ratio of natural gas and the potassium content of source rock (Shen et al., 1995):

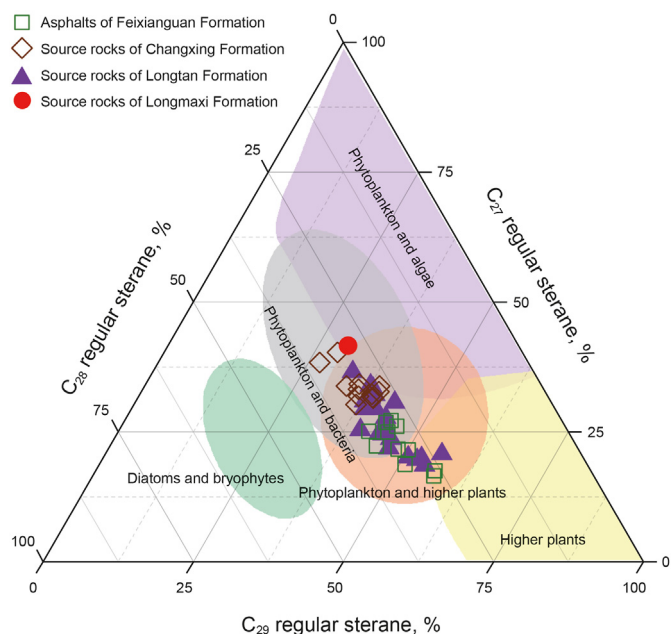


Fig. 9. Comparison of $\alpha\alpha\alpha 20R-C_{27}$, C_{28} and C_{29} regular steranes between reservoir asphalts of the Feixianguan Formation, Eastern Sichuan Basin and source rocks of Upper Permian (based on Huang and Meinschein, 1979); the Silurian source rock data from Li et al. (2016).

$$T = 0.0574 \times ({}^{40}\text{Ar}/{}^{36}\text{Ar}) / (K \times 100) + 190 \quad (2)$$

where *K* is the potassium content of the source rock, %, *T* is the stratum age of the source rock, Ma, and ${}^{40}\text{Ar}/{}^{36}\text{Ar}$ is the ${}^{40}\text{Ar}/{}^{36}\text{Ar}$ value of the natural gas.

According to the calculation, the ages of natural gas-source rocks in the study area are 263.41–241.78 Ma, and the corresponding geological age of each sample is consistent with that of the Longtan Formation (256–240 Ma) (Table 2 and Fig. 11). It was further confirmed that the main natural gas source of the Feixianguan Formation in the ESB was the argillaceous source rock of the Longtan Formation.

5.2.4. Comprehensive analysis of gas source

In summary, the potential source rock of natural gas in the Feixianguan Formation was revealed from the perspective of gas-gas comparison. Then, based on the inheritance effect of organic molecular of biomarkers, the main source rock was indirectly revealed by reservoir asphalt. Finally, the above viewpoint was further confirmed quantitatively by noble gas chronology. Based on the principle of priority and mutual confirmation, it was comprehensively concluded that the main gas source of the Feixianguan Formation was mudstone source rocks in the Permian Longtan Formation.

5.3. Natural gas accumulation model

Based on parameters such as the stratum thickness, thickness and TOC of the source rock, thermal history and current geothermal field, and taking Well PG 2 as an example, the burial and thermal

history and the hydrocarbon generation and expulsion history were simulated for the argillaceous source rock of the Upper Permian Longtan Formation by using BasinMod 1D. Combined with the oil and gas geological conditions and tectonic evolution history in the study area, the coupling relationships and spatiotemporal configurations of key accumulation events were established for Feixianguan Formation natural gas (Fig. 12). According to the current seismic profile, the oil and gas accumulation model was further established for the Feixianguan Formation in the ESB (Fig. 13).

Most marine strata in the ESB have entered the overmature stage, and paleo-gas reservoirs were formed by the high-temperature cracking of paleo-oil reservoirs (Liu et al., 2020). The high-steep structural belt in the ESB is located on the east side of the Huayingshan fault zone and the west side of the Qiyueshan fault zone. The structure is complex, and the source-reservoir fault is developed. The fault is broken down to the Silurian and up to the Jialingjiang Formation, which provides a good channel for oil and gas migration (Cai, 2016). Along the platform margin belt of the east and west sides of the “Kaijiang-Liangping” trough, reef and beach reservoirs of the Feixianguan Formation in the ESB developed in banded and clumped distributions. The scale of high-quality reservoirs was developed and has good reservoir space. The upper Jialingjiang Formation and Leikoupo Formation have developed a large set of gypsum-salt caprocks, which have a very strong sealing ability and seal effectively (Liu et al., 2020). The source rocks of the Upper Permian Longtan Formation entered the threshold of hydrocarbon generation in the Late Triassic and entered the peak of oil generation in the Early Jurassic, with high oil generation intensity (Fig. 12). During the Late Indosinian-Early and Middle Yanshanian, the structural-lithologic traps developed in the Feixianguan Formation were important accumulation areas for ancient oil and gas reservoirs (Ma, 2008).

The process for accumulation of natural gas in the Feixianguan Formation in the ESB has gone through four stages: (1) During the Middle-Late Triassic, the palaeo-uplift was basically formed under the influence of the Indosinian movement. At this time, the argillaceous source rocks in the upper Permian Longtan Formation entered the threshold of oil generation and began to generate oil but did not begin to expel oil. (2) In the Early Jurassic, the overall inheritance of the paleo-uplift developed, and a large number of dissolution pores and early fractures developed in the Feixianguan Formation. At this time, the argillaceous source rocks of the Longtan Formation entered the peak period of oil generation and expulsion, and the generated crude oil migrated upwards along the source-reservoir fault to the reservoirs of the Feixianguan Formation. The structural heights of the paleo-uplift effectively captured liquid hydrocarbons from horizontal and vertical directions, forming the paleo-oil reservoirs of the Feixianguan Formation. (3) In the middle-Late Jurassic, the paleo-uplift was inherited and developed, the basin was rapidly subsiding, and the source rock entered the overmature stage. When the reservoir temperature of the Feixianguan Formation paleo-reservoirs reached 160 °C, the liquid hydrocarbons of the paleo-oil reservoirs began to undergo thermal cracking, and this continued until the reservoir temperature exceeded 200 °C. The generated oil-cracked gases gradually migrated and accumulated at the high parts along the faults and fractures and formed paleo-gas reservoirs. (4) Since the Jurassic and affected by the Yanshan-Himalayan orogenic movement, the strata in the ESB have been uplifted and eroded. The paleo-uplift began to disintegrate, and a large number of fractures developed in the late stages. Under the control of the fluid dredging system and the current structural features, the paleo-gas reservoirs were enriched in the current structural-lithologic composite traps and formed the current natural gas reservoirs.

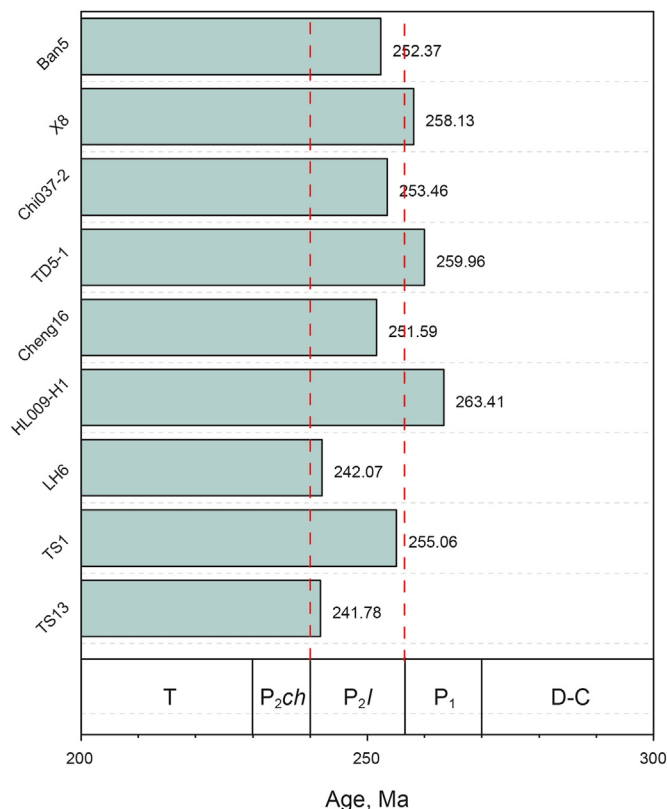


Fig. 11. The distribution of the geological age of gas-source in the Feixianguan Formation, Eastern Sichuan Basin
 T = Triassic; P_{2ch} = Changxing Formation; P_{2l} = Longtan Formation; P₁ = Lower Permian; D = Devonian; C = Carboniferous.

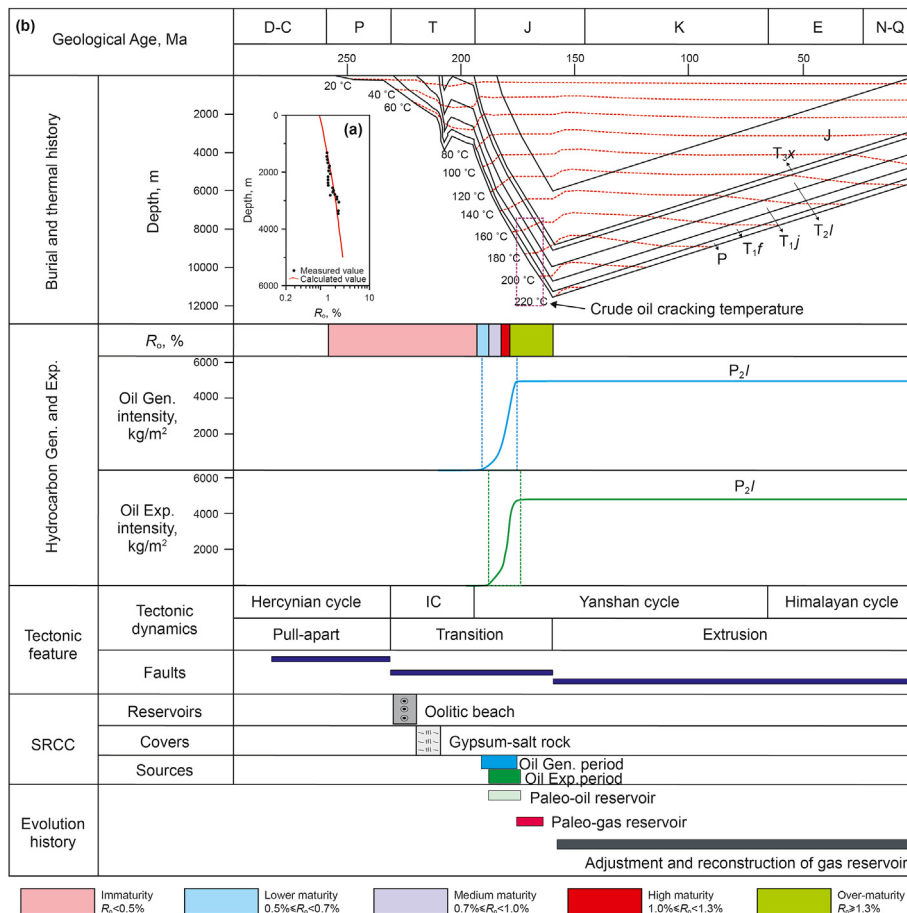


Fig. 12. Gas accumulation event map in the Feixiang Formation, Eastern Sichuan Basin
 SRCC = source-reservoir-cap combination; IC = Indosinian cycle; J = Jurassic; P = Permian; K = Cretaceous; E = Palaeogene; N-Q = Neogene-Quaternary; T_{3x} = Xujiahe Formation; T_{2l} = Leikoupo Formation; T_{1j} = Jialingjiang Formation; T_{1f} = Feixiang Formation.

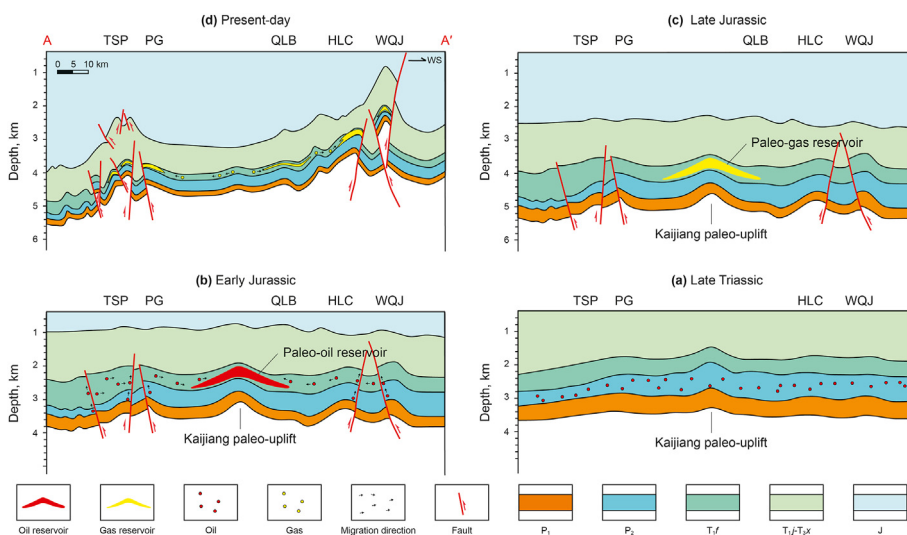


Fig. 13. Diagram of gas reservoirs forming process in the Feixiang Formation, Eastern Sichuan Basin.

6. Conclusions

(1) The H₂S-rich and H₂S-poor gas reservoirs of the Feixiang Formation are distributed on the east and west sides of the

Kaijiang-Liangping trough in the ESB, respectively. The carbon and hydrogen isotope compositions of the natural gas in the gas reservoirs are generally heavy and have the typical characteristics of high-maturity dry gas reservoirs. However,

the hydrocarbon compositions and hydrocarbon isotope compositions of the two are quite different. The content of hydrocarbon components in the H₂S-rich gas reservoirs is significantly lower, the drying coefficient is higher, and the ethane hydrocarbon isotopes are heavier.

- (2) According to a comprehensive assessment of hydrocarbon gas and nonhydrocarbon gas, the natural gas of the Feixianguan Formation is organic thermogenic gas, which is mainly oil-type gas generated by secondary cracking of crude oil. The gas-generating parent material is mainly type II kerogen.
- (3) Through comparative analyses of natural gas-natural gas, reservoir asphalt-source rock and natural gas-source rock relationships, it is revealed that the natural gas of the Feixianguan Formation in the ESB was mainly generated by the argillaceous source rocks of the Upper Permian Longtan Formation.
- (4) The process for natural gas accumulation in the Feixianguan Formation was as follows: the source rock of the Longtan Formation of the Upper Permian entered the oil generation threshold in the Late Triassic and entered the oil generation peak in the Early Jurassic, and then the crude oil migrated to the paleo-structural heights of the Feixianguan Formation to form the paleo-oil reservoirs. During the Middle-Late Jurassic, the basin rapidly subsided. The paleo-oil reservoirs were pyrolyzed to form paleo-gas reservoirs when the temperature exceeded 160 °C. Since the end of the Late Jurassic, the paleo-gas reservoirs have entered a stage of adjustment and finalization and formed the present natural gas reservoirs.

Declaration of competing interest

The authors declare that they have no known competing financial interests or personal relationships that could have appeared to influence the work reported in this paper.

Acknowledgments

This work was supported by the National Natural Science Foundation of China (Grant No. 41972109) and the Chengdu University of Technology Postgraduate Innovative Cultivation Program (CDUT2022BJCX004).

Abbreviation

ESB	Eastern Sichuan Basin
GC	gas chromatography
MS	mass spectrometry

Appendix A. Supplementary data

Supplementary data to this article can be found online at <https://doi.org/10.1016/j.petsci.2023.02.005>.

References

Bernard, B.B., Brooks, J.M., Sackett, W.M., 1976. Natural gas seepage in the Gulf of Mexico. *Earth Planet Sci. Lett.* 31, 48–54. [https://doi.org/10.1016/0012-821X\(76\)90095-9](https://doi.org/10.1016/0012-821X(76)90095-9).

Battani, A., Sarda, P., Prinzhofer, A., 2000. Basin scale natural gas source, migration and trapping traced by noble gases and major elements: the Pakistan Indus basin. *Earth Planet Sci. Lett.* 81, 229–249. [https://doi.org/10.1016/S0012-821X\(00\)00188-6](https://doi.org/10.1016/S0012-821X(00)00188-6).

Barry, P.H., Kulongoski, J.T., Landon, M.K., et al., 2018. Tracing enhanced oil recovery signatures in casing gases from the Lost Hills oil field using noble gases. *Earth Planet Sci. Lett.* 496, 57–67. <https://doi.org/10.1016/j.epsl.2018.05.028>.

Cai, C.F., Zhang, C.M., He, H., et al., 2013. Carbon isotope fractionation during methane-dominated TSR in East Sichuan Basin gas fields, China: a review (Review). *Mar. Petrol. Geol.* 48, 100–110. <https://doi.org/10.1016/j.marpetgeo.2022.105892>.

Cai, X.Y., 2016. *Sichuan Basin Natural Gas Dynamic Accumulation*. Science Press, Beijing, p. 467 pp (In Chinese).

Chen, J.P., Wang, X.L., Sun, Y.G., et al., 2021. Factors controlling natural gas accumulation in the southern margin of Junggar Basin and potential exploration targets. *Front. Earth Sci.* 9, 635230. <https://doi.org/10.3389/feart.2021.635230>.

Choi, J., Kim, J.H., Torres, M.E., et al., 2013. Gas origin and migration in the Ulleung basin, east sea: results from the Second Ulleung basin gas hydrate drilling expedition (UBGH2). *Mar. Petrol. Geol.* 47, 113–124. <https://doi.org/10.1016/j.marpetgeo.2013.05.022>.

Dai, J.X., 1985. Distribution characteristics, classification and genesis of natural gas containing hydrogen sulfide in China, 04 *Acta Sedimentol. Sin.* 109–120 (In Chinese).

Galimov, E.M., 1988. Sources and mechanism of formation of gaseous hydrocarbons in sedimentary rocks. *Chem. Geol.* 71, 77–95. [https://doi.org/10.1016/0009-2541\(88\)90107-6](https://doi.org/10.1016/0009-2541(88)90107-6).

Hao, F., Guo, T.L., Du, C.G., et al., 2009. Accumulation mechanisms and evolution history of the giant Puguang gas field, Sichuan Basin, China. *Acta Geol. Sin.* 83, 136–145.

Hu, P.A., 2009. *Study on Organic Petrology and Organic Geochemistry of High Hydrogen Sulfide Gas Reservoirs in Feixianguan Formation, Northeast Sichuan*. Zhejiang University, China, thesis, p. 150 pp (In Chinese).

Hu, G.Y., Yu, C., Gong, D.Y., et al., 2014. The origin of natural gas and influence on hydrogen isotope of methane by TSR in the upper Permian Changxing and the lower triassic Feixianguan formations in northern Sichuan Basin, SW China. *Energy Explor. Exploit.* 32, 139–158. <https://doi.org/10.1260/0144-5987.32.1.139>.

Huang, W.Y., Meinschein, W.G., 1979. Sterols as ecological indicators. *Geochem. Cosmochim. Acta* 43, 739–745. [https://doi.org/10.1016/0016-7037\(79\)90257-6](https://doi.org/10.1016/0016-7037(79)90257-6).

Hu, T., Pang, X.Q., Jiang, F.J., et al., 2022. Dynamic continuous hydrocarbon accumulation (DCHA): existing theories and a new unified accumulation model. *Earth Sci. Rev.* 232, 104109. <https://doi.org/10.1016/j.earscirev.2022.104109>.

Jenden, P.D., Newell, K.D., Kaplan, I.R., et al., 1988. Composition and stable-isotope geochemistry of natural gases from Kansas. Midcontinent, U.S.A. *Chem. Geol.* 71, 117–147. [https://doi.org/10.1016/0009-2541\(88\)90110-6](https://doi.org/10.1016/0009-2541(88)90110-6).

Kotarba, M.J., Wieclaw, D., Dziadzio, P., et al., 2014. Organic geochemical study of source rocks and natural gas and their genetic correlation in the eastern part of the Polish Outer Carpathians and Palaeozoic-Mesozoic basement. *Mar. Petrol. Geol.* 56, 97–122. <https://doi.org/10.1016/j.marpetgeo.2014.03.014>.

Li, J., Zhou, S.X., Fu, D.L., et al., 2016. Oil-source rock correlation for paleo-oil reservoir in the Puguang gas field, Northeast Sichuan Basin, Southwest China. *Petrol. Sci. Technol.* 34, 578–586. <https://doi.org/10.1080/10916466.2016.1160113>.

Li, Q.Q., Li, B.B., Xu, S., et al., 2020. Source and accumulation processes of natural gases in the Qixia Formation in the northwestern Sichuan Basin, SW China. *J. Pet. Sci. Eng.* 198, 108236. <https://doi.org/10.1016/j.petrol.2020.108236>.

Li, Y., Chen, S.J., Wang, Y.X., et al., 2019. The origin and source of the Devonian natural gas in the northwestern Sichuan Basin, SW China. *J. Pet. Sci. Eng.* 181, 1–10. <https://doi.org/10.1016/j.petrol.2019.106259>.

Liu, B., He, S., Meng, L., et al., 2021a. Sealing mechanisms in volcanic faulted reservoirs in Xujiaweizi extension, northern Songliao basin, northeastern China. *AAPG (Am. Assoc. Pet. Geol.) Bull.* 105, 1721–1743. <https://doi.org/10.1306/03122119048>.

Liu, Q.Y., Worden, R.H., Jin, Z.J., et al., 2014. Thermochemical sulphate reduction (TSR) versus maturation and their effects on hydrogen stable isotopes of very dry alkane gases. *Geochem. Cosmochim. Acta* 137, 208–220. <https://doi.org/10.1016/j.gca.2014.03.013>.

Liu, Q.Y., Wu, X.Q., Wang, X.F., et al., 2019. Carbon and hydrogen isotopes of methane, ethane, and propane: a review of genetic identification of natural gas. *Earth Sci. Rev.* 190, 247–272. <https://doi.org/10.1016/j.earscirev.2018.11.017>.

Liu, S.G., Deng, B., Sun, W., et al., 2020. Is Sichuan Basin a 'super' petroliferous basin? *J. Xihua Univ. (Nat. Sci. Ed.)* 39, 20–35 (In Chinese with English abstract).

Liu, S.G., Sun, W., Song, J.M., et al., 2015. Tectonics-controlled distribution of marine petroleum accumulations in the Sichuan Basin, China. *Earth Sci. Front.* 3, 146–160. <https://doi.org/10.13745/j.esf.2015.03.013> (In Chinese with English abstract).

Liu, S.G., Yang, Y., Deng, B., et al., 2021b. Tectonic evolution of the Sichuan Basin, Southwest China. *Earth Sci. Rev.* 213, 103470. <https://doi.org/10.1016/j.earscirev.2020.103470>.

Liu, W.H., Wang, J., Tenger, et al., 2012. Multiple hydrocarbon generation of marine strata and its tracer technique in China. *Acta Pet. Sin.* 201, 115–125 (In Chinese with English abstract).

Liu, W.H., Xu, Y.C., 1993. Characteristics of helium and argon isotope composition in natural gas. *Sci. Rep.* 38, 818–821 (In Chinese).

Loomer, D.B., Macquarrie, K.T.B., Al, T.A., 2020. Comparison of isotopic compositions of hydrocarbon gas in shallow groundwater and a deep oil and natural gas reservoir in southeastern New Brunswick, Canada. *Atl. Geol.* 56, 207–229. <https://doi.org/10.4138/atlgol.2020.009>.

Luo, Q.Y., Hao, J.Y., Li, K.W., et al., 2019. A new parameter for the thermal maturity assessment of organic matter from the Lower Palaeozoic sediments: a re study on the optical characteristics of graptolite periderms. *Acta Geol. Sin.* 93 (9), 2362–2371. <https://doi.org/10.19762/j.cnki.dizhixuebao.2019192> (In Chinese).

- with English abstract).
- Lu, J., Ma, J., Chen, S.J., et al., 2017. The geochemistry and origin of lower Permian gas in the northwestern Sichuan basin, SW China. *J. Pet. Sci. Eng.* 157, 906–916. <https://doi.org/10.1016/j.petrol.2017.07.068>.
- Ma, A.L., Li, H.L., Li, J.H., et al., 2020. Geochemical characteristics of Middle-Upper Ordovician source rocks in the Kalpin outcrop profiles and marine oil-source correlation, Tarim Basin, NW China. *J. Nat. Gas Geosci.* 5, 143–155. <https://doi.org/10.1016/j.jnggs.2020.04.001>.
- Ma, Y.S., 2008. Geochemical characteristics and sources of natural gas in Puguang gas field. *Nat. Gas Geosci.* 1, 1–7 (In Chinese).
- Machel, H.G., Krouse, H.R., Roger, S., 1995. Products and distinguishing criteria of bacterial and thermochemical sulfate reduction. *Appl. Geochem.* 10, 373–389. [https://doi.org/10.1016/0883-2927\(95\)00008-8](https://doi.org/10.1016/0883-2927(95)00008-8).
- Magoon, L.B., Peters, E.P., Hudson, L.H., 2005. Egret-Hibernia(!), a significant petroleum system, northern Grand Banks area, offshore eastern Canada. *AAPG (Am. Assoc. Pet. Geol.) Bull.* 89, 1203–1237. <https://doi.org/10.1306/05040504115>.
- Pang, X.Q., Zhu, W.L., Lu, X.X., et al., 2015. A study on hydrocarbon thresholds controlling reservoir accumulation and predictive evaluation of favorable accumulation areas in eastern Bohai Bay Basin. *Petrol. J.* 36, 43483. <https://doi.org/10.7623/syxb201552001> (In Chinese with English abstract).
- Prinzhofer, A.A., Huc, A.Y., 1995. Genetic and post-genetic molecular and isotopic fractionations in natural gases. *Chem. Geol.* 126, 281–290. [https://doi.org/10.1016/0009-2541\(95\)00123-9](https://doi.org/10.1016/0009-2541(95)00123-9).
- Rooney, M.A., Claypool, G.E., Chung, H.M., 1995. Modeling thermogenic gas generation using carbon isotope ratios of natural gas hydrocarbons. *Chem. Geol.* 12, 219–232. [https://doi.org/10.1016/0009-2541\(95\)00119-0](https://doi.org/10.1016/0009-2541(95)00119-0).
- Saadati, H., Al-Iessa, H.J., Alizadeh, B., et al., 2016. Geochemical characteristics and isotopic reversal of natural gases in eastern Kopeh-Dagh, NE Iran. *Mar. Petrol. Geol.* 78, 76–87. <https://doi.org/10.1016/j.marpetgeo.2016.09.004>.
- Schoell, M., 1980. The hydrogen and carbon isotopic composition of methane from natural gases of various origins. *Geochem. Cosmochim. Acta* 44 (5), 649–661. [https://doi.org/10.1016/0016-7037\(80\)90155-6](https://doi.org/10.1016/0016-7037(80)90155-6).
- Shen, P., Xu, Y.C., Liu, W.H., et al., 1995. Applied models of rare gas geochemistry in the research of natural gases. *Acta Sedimentol. Sin.* 13, 48–58 (In Chinese).
- Song, J.Y., Chen, T., Zhang, J.L., 2022. Permian and triassic hydrocarbon migration and accumulation in the Cainan area, Junggar basin, China. *J. Pet. Sci. Eng.* 210. <https://doi.org/10.1016/j.petrol.2021.109965>, 0920–4105.
- Spaak, G., Edwards, D.S., Foster, C.C., et al., 2020. Geochemical characteristics of early Carboniferous petroleum systems in Western Australia. *Mar. Petrol. Geol.* 113, 104073. <https://doi.org/10.1016/j.marpetgeo.2019.104073>.
- Wang, X.B., Zou, C.N., Li, J., et al., 2019. Comparison on Rare Gas Geochemical Characteristics and Gas Originations of Kuche and Southwestern Depressions in Tarim Basin, China. *Geofluids* 1–15. <https://doi.org/10.1155/2019/1985216>, 2019.
- Wu, X.Q., Chen, Y.B., Zhai, C.B., et al., 2020. Gas source and exploration direction of the middle triassic Leikoupo Formation in the Sichuan Basin, China. *J. Nat. Gas Geosci.* 5, 317–326. <https://doi.org/10.11764/j.issn.1672-1926.2020.05.015>.
- Wu, X.Q., Liu, G.X., Liu, Q.Y., et al., 2016. Geochemical characteristics and genetic types of natural gas in the Changxing-Feixianguan Formations from the Yuanba gas field in the Sichuan Basin, China. *Nat. Gas Geosci.* 26 (11), 2155–2165. <https://doi.org/10.11764/j.issn.1672-1926.2015.11.2155>.
- Wu, X.Q., Liu, Q.Y., Liu, G.X., et al., 2019. Genetic types of natural gas and gas-source correlation in different strata of the Yuanba gas field, Sichuan Basin, SW China. *J. Asian Earth Sci.* 181, 103906. <https://doi.org/10.1016/j.jseas.2019.103906>.
- Xie, Z.Y., Li, Z.H., Wei, G.Q., et al., 2016. Experimental research on the potential of sapropelic kerogen cracking gas and discrimination of oil cracking gas. *Nat. Gas Geosci.* 6, 1057–1066. <https://doi.org/10.11764/j.issn.1672-1926.2016.06.1057> (In Chinese with English abstract).
- Yang, J.J., Wang, Y.G., Wang, L.S., et al., 2002. The origin of natural gases and geochemistry characters of Changxing reef and Feixianguan oolitic beach gas reservoirs in Eastern Sichuan Basin. *Acta Sedimentol. Sin.* 2, 349–353 (In Chinese with English abstract).
- Yang, M.H., Zuo, Y.H., Zhang, J.Z., et al., 2021. Hydrocarbon kitchen evolution in the early Cretaceous Bayingebi 2 Formation in the Chagan depression, Yingen-Ejinaqi basin, north Central China. *ACS Omega* 6, 12194–12204. <https://doi.org/10.1021/acsomega.1c00944>.
- Zhang, S.C., Zhu, G.Y., Chen, J.P., et al., 2007. A discussion on gas sources of the Feixianguan Formation H₂S-rich giant gas fields in the northeastern Sichuan Basin. *Sci. Bull.* 101, 113–124. <https://doi.org/10.1007/s11434-007-6014-8>.
- Zhang, S.C., He, K., Hu, G.Y., et al., 2018. Unique chemical and isotopic characteristics and origins of natural gases in the Paleozoic marine formations in the Sichuan Basin, SW China: isotope fractionation of deep and high mature carbonate reservoir gases. *Mar. Petrol. Geol.* 89, 68–82. <https://doi.org/10.1016/j.marpetgeo.2017.02.010>.
- Zhao, W.Z., Xu, C.C., Wang, T.S., 2011. Comparative study of gas accumulations in the Permian Changxing reefs and triassic Feixianguan oolitic reservoirs between Longgang and LuoJiazhai-Puguang in the Sichuan Basin. *Chin. Sci. Bull.* 56, 3310–3320.
- Zheng, Z.Y., Zuo, Y.H., Jiang, S., et al., 2020. Carbon isotope kinetics effect on the natural gas accumulation: a case study of the Baimiao area, Dongpu Depression, North China. *Energy Fuels* 4, 1608–1619. <https://doi.org/10.1021/acs.energyfuels.9b03820>.
- Zheng, Z.Y., Zuo, Y.H., Wen, H.G., et al., 2023. Natural gas characteristics and gas-source comparisons of the lower triassic Jialingjiang Formation, eastern Sichuan Basin. *J. Pet. Sci. Eng.* 221, 111165. <https://doi.org/10.1016/j.petrol.2022.111165>.
- Zhu, Y.M., Gu, S.X., Li, Y., et al., 2012. Biological organic source and depositional environment of over-mature source rocks of Longtan Formation in Sichuan basin. *Geochimica* 41, 35–44 (In Chinese with English abstract).
- Zuo, Y.H., Qiu, N.S., Zhang, Y., et al., 2011. Geothermal regime and hydrocarbon kitchen evolution of the offshore Bohai Bay Basin, North China. *AAPG (Am. Assoc. Pet. Geol.) Bull.* 95, 749–769. <https://doi.org/10.1306/09271010079>.